3,4,5-Trimethoxy Substitution on an N-DMBI Dopant with New N-type Polymers: Polymer-Dopant Matching for Improved Conductivity-Seebeck Coefficient Relationship

Jinfeng Han[1], Arlene Chiu[2], Connor Ganley[3], Patty McGuiggan[1], Susanna M. Thon[2], Paulette Clancy[3], Howard E. Katz[1,*]

[1]Department of Materials Science and Engineering, Johns Hopkins University, 3400 North Charles Street, Baltimore, Maryland 21218, United States

[2]Department of Electrical and Computer Engineering, Johns Hopkins University, 3400 North Charles Street, Baltimore, Maryland 21218, United States[2]

[3]Department of Chemical and Biomolecular Engineering, Johns Hopkins University, Baltimore, Maryland 21218, United States.

Abstract: Achieving high electrical conductivity and thermoelectric power factor simultaneously for n-type organic thermoelectrics is still challenging. By constructing two new acceptor-acceptor n-type conjugated polymers with different backbones and introducing the 3,4,5-trimethoxyphenyl group to form the new n-type dopant 1,3-dimethyl-2-(3,4,5-trimethoxyphenyl)-2,3-dihydro-1H-benzo[d]imidazole (TP-DMBI), high electrical conductivity of 11 S cm^{-1} and power factor of 32 μW m^{-1} K^{-2} are achieved. Calculations using Density Functional Theory show that TP-DMBI presents a higher singly occupied molecular orbital (SOMO) energy level of -1.94 eV than that of the common dopant 4-(1, 3-dimethyl-2, 3-dihydro-1H-benzoimidazol-2-yl) phenyl) dimethylamine (N-DMBI) (-2.36 eV), which can result in a larger offset between the SOMO of dopant and lowest unoccupied molecular orbital (LUMO) of n-type polymers, though that effect may not be dominant in the present work. The doped polymer films exhibit higher Seebeck coefficient and power factor than films using N-DMBI at the same doping levels or similar electrical conductivity levels. Moreover, TP-DMBI doped polymer films offer much higher electron mobility of up to 0.53 cm^2 V^{-1} s^{-1} than films with N-DMBI doping, demonstrating the potential of TP-DMBI, and 3,4,5-trialkoxy DMBIs more broadly, for high performance n-type organic thermoelectrics.

1. Introduction

Organic (semi)conducting materials have attracted increasing attention in academia and industry because of the potential applications in energy conversion, optoelectronics, organic thin film transistors (OTFTs) and disease detection and treatment.[1] Doping is a common and effective way to increase the conductance of organic electronic devices, for example OTFTs[2] and organic thermoelectric devices (OTEs).[3] Thanks to the appealing advantages of mechanical flexibility and nontoxicity,[4] organic thermoelectrics, especially polymer thermoelectrics, are under consideration for wearable devices. Both p-type[5] and n-type[6] organic thermoelectrics usually show inherently low thermal conductivity (κ: 0.2-0.5 W m^{-1} K^{-1}), beneficial for a high figure of merit *ZT*. Power factor (*PF*), which varies considerably more, is more generally used to evaluate organic thermoelectrics, and is defined by the equation $PF = S^2\sigma$, where S and σ are the Seebeck coefficient and electrical conductivity, respectively. Hence, high electrical conductivity is indispensable for high power factor. Recently, high p-type σ of over 300 S cm^{-1} has been reported for polythiophene derivatives[7] and donor-acceptor (D-A) polymer thermoelectrics.[8] Moreover, ultrahigh p-type σ of over 2000 S cm^{-1} and power factor of 1270 μW m^{-1} K^{-2} have been demonstrated previously in electrochemically oxidized PEDOT films.[9] Similar electrical conductivity and power factors of n-type and p-type organic thermoelectrics are required to generate electricity efficiently from multidevice modules. Due to the poor air-stability and low electronic mobility, most n-type devices present σ of less than 10 S cm^{-1},[10] or even below 1 S cm^{-1}.[11] Therefore, developing new polymers and dopants for n-type organic thermoelectrics is still a pressing endeavor.

Engineering of polymer backbones is a logical way to enhance carrier density and electron mobilities, such as by increasing electron affinity by raising conjugation length[12] and electron-withdrawing capabilities of acceptor units,[13] constructing rigid polymers,[6, 14] designing acceptor-acceptor (A-A) polymers to decrease lowest unoccupied molecular orbital (LUMO) energy levels[15] and modifying donor units to become more electron-withdrawing.[16] Tuning the branching point has also been helpful for achieving high conductivity values.[17] For high electrical conductivity, high doping levels are usually required, and this results in lower Seebeck coefficient. The compatibility of polymers and dopants plays a key role in carrier transport and generation of thermoelectric potential.[18] For organic thermoelectrics, mild doping can enhance the carrier density and mobilities, but usually not sufficiently to achieve high conductivity. On the other hand, heavy doping will disorder the polymer morphology, which can lead to low carrier mobility.[14b] It has been shown that reasonable matching of host-polymer and n-type dopant can enable high electrical conductivity and high power factor simultaneously.[19]

Here, we used a newly synthesized n-type dopant, TP-DMBI, with two new acceptor-acceptor polymers, PClBD and PDTz, and compare their thin film electrical conductivity, electron mobility, energy levels and morphologies when mixed with the new dopant as well as the common commercial n-dopant N-DMBI. The core acceptor groups of the new polymers are the same as in our previous work[16a] but have more decidedly electron-accepting linkers that we hypothesized would further promote doping. TP-DMBI is the first 3,4,5-trialkoxy N-DMBI synthesized or used as an n-dopant, though the less planar 2,4,6-trimethoxy compound was used in a polymer-carbon nanotube doped composite,[20] and thus represents a prototype for increasing electron donation and polymer compatibility. The electron mobility (μ_e) of 0.8 mol%

TP-DMBI doped PClBD, PDTz and the 1:1 PClBD:PDTz mixture are 0.51±0.02, 0.44±0.04 and 0.45±0.06 $cm^2 V^{-1} s^{-1}$, respectively, which are all much higher than pristine and N-DMBI doped thin films, suggesting the effective doping capability. The highest *PF* and σ of TP-DMBI doped PClBD and PDTz are 32 μW $m^{-1} K^{-2}$ and 11 S cm^{-1}, respectively, which are among the highest performances reported in n-type conjugated polymer thermoelectrics. Moreover, TP-DMBI doped polymers exhibit higher Seebeck coefficient than N-DMBI doped at similar conductivity levels. The results demonstrate the use of A-A type polymers and TP-DMBI dopant for high-performance n-type organic thermoelectrics.

2. Results and Discussion

A-A type polymers should accept electrons from dopants more readily than donor-acceptor polymers because the two acceptor moieties should synergistically contribute electron-demanding character. In addition, the ratios of rotatable single bonds connecting two moieties in polymers also play a key role in electrical conductivity. Here, two n-type conjugated polymers were synthesized by employing the strong electron-withdrawing acceptor units of halogenated BDOPV as building blocks.

An A-A type polymer PClBD was synthesized by Stille coupling of halogenated BDOPV and trimethyltin substituted acceptor unit diketopyrrolopyrrole (DPP). The molecular weight was 125.5 kDa and polydispersity index was 2.1 (Figure S1 and Table S1). Polymer PDTz was synthesized by coupling with a halogenated BDOPV and unit bithiazole. The molecular weight was 39.0 kDa and the polydispersity was 2.1 (Figure S2 and Table S1). Both polymers can be dissolved in chloroform, toluene, chlorobenzene and ortho-dichlorobenzene (*o*-DCB). There are two and one single

bonds for DPP and bithiazole, respectively, so the ratio of single bonds in PClBD is larger than that in PDTz. TP-DMBI was synthesized by aldimine condensation of N^1,N^2-dimethylbenzene-1,2-diamine and 3,4,5-trimethoxybenzaldehyde with simple sonication at a high yield of 92%. We found the color of TP-DMBI solution in *o*-DCB was unchanged after storing in the glove box for half a year, while the color of N-DMBI solution changed from colorless to faint yellow.

The energy levels of the pristine and doped polymer films were determined by cyclic voltammetry (CV) with Ag/Ag^+ as the reference electrode. As shown in **Figure 1**, PClBD and PDTz display low LUMO energy levels of -4.17 and -4.32 eV, both of which are higher than the highest occupied molecular orbital (HOMO) energy levels of N-DMBI (-4.70 eV)[21] and TP-DMBI (-4.53 eV).[22] Thus, the doping process requires cleaving the tertiary C-H bond of the dopants. The HOMO energy levels of PClBD and PDTz are -5.28 and -6.07 eV, respectively. The corresponding band gaps are 1.11 and 1.75 eV, suggesting PClBD is a typical low-band gap polymer. PDTz has a low LUMO energy level and wide band gap similar to other n-type polymers containing the bithiazole unit.[23] PDTz also appears to have broader initial electrochemical reduction peaks, possibly indicating a broader range of trap structures and energies. To check the effect of various doping levels on energy levels of polymer films, cyclic voltammetry of PClBD and PDTz films doped with 10 mol%, 50 mol% and 100 mol% of N-DMBI and TP-DMBI was investigated, and are shown in **Figure 1**, Figure S3, and Table S2. Only minor fluctuations were observed.

Ab initio calculations of SOMO energy levels were conducted on the N-DMBI$^{\cdot}$ and TP-DMBI$^{\cdot}$ radicals. We used Koopmans' theorem in conjunction with subtractive quantification of the ionization potential.[11c, 24] The SOMO energy levels were found

to be -2.36 and -1.94 eV, respectively. The SOMO energy levels of N-DMBI˙ are similar with reported works.[21, 25] The higher-lying SOMO energy levels of TP-DMBI can result in a larger offset between the SOMO of dopant and LUMO of n-type polymers and could give a higher doping efficiency than N-DMBI where electronic driving force is the limiting factor.[25b, 26] However, the driving force for electron transfer from the SOMO to the polymers, approximately 2 eV, is high enough that dopant-polymer distance, dielectric constant of material between dopant and polymer, or kinetics of dopant radical dimerization could be more important determinants of doping efficiency. These would all depend on detailed local structures formed by each composition.

The UV-vis-NIR absorption spectra of pristine and doped polymer films are displayed in **Figure 2**. The π-π* transition contributes to two absorption peaks for pristine PClBD at wavelengths shorted than 600 nm, and there is no π-π* transition peak detected for PDTz because it is covered by intramolecular charge transfer absorption in the low-energy region.[27] PClBD exhibits a wider absorption spectrum than PDTz with an absorption onset of 1178 nm due to the stronger intramolecular charge transfer. The optical band gaps of PClBD and PDTz are 1.05 and 1.44 eV, consistent with the band gaps calculated from redox potentials. The neutral absorptions of PClBD and PDTz were bleached when the films were doped by N-DMBI and TP-DMBI, and new peaks appear at 1340-1620 and 900-1200 and 1380-1740 nm for PClBD and PDTz which can be assigned to polaron/bipolaron transitions[28] and charge transfer states.[29] The intensity ratios of absorption bands at 700-1000 and 1340-1620 nm for N-DMBI and TP-DMBI doped PClBD are 3.80 and 2.25, respectively (**Figure 2a**). This indicates that TP-DMBI doped PClBD films have higher doping levels under the same conditions.[30] The intensity ratios of N-DMBI and TP-DMBI doped PDTz absorption

bands at 550-800 and 900-1200 nm are 2.00 and 1.49, again indicating that doping with TP-DMBI gave relatively more intense polaron/bipolaron peaks (**Figure 2b**). The absorption intensity ratios of mixtures of PClBD and PDTz doped with N-DMBI and TP-DMBI also show similar phenomena (Figure S4). The absorption intensity ratios of 30, 75 and 100 mol% N-DMBI and TP-DMBI doped polymers showed similar trends with 50 mol% N-DMBI and TP-DMBI doped polymer films (Figure S5). The absorption spectra taken together indicate that TP-DMBI can be an efficient n-dopant for n-type organic thermoelectrics and can at least compete with N-DMBI.

Electron paramagnetic resonance (EPR) spectroscopy was used to estimate the free radical presence and number of spins in doped solutions and films. As shown in **Figure 2**, both N-DMBI and TP-DMBI doped PClBD and PDTz exhibit high EPR intensity over a range of dopant concentrations, saturating at about 75% dopant mole fraction (moles of dopant/moles of polymer repeat unit) with TP-DMBI giving much higher intensity at 10% dopant mole fraction, and the PClBD-N-DMBI combination showing the most dopant concentration dependence of the EPR signal. The measured spin intensity may not all be from single electron charge carriers because of other side reactions.[21, 31] Polymer films doped by N-DMBI and TP-DMBI show strong radical signals which further confirms the efficient doping (Figure S6).

Doped polymer films were prepared by drop-casting the mixed solution of polymers and dopants onto glass substrates with prepatterned gold electrodes. The σ and S of doped polymer films were determined by a four-point-probe method and detecting the thermoelectric voltages under temperature gradients (ΔT), respectively. To optimize the performance of devices, polymers were doped with different mole fractions. All of the doped polymer films with dopant concentrations above 30 mol% show reasonably high

n-type σ of over 2 S cm^{-1},[32] especially at the dopant mole fractions of 50 and 75 mol% (**Figure 3**). PDTz doped with 75 mol% TP-DMBI exhibits a maximum σ of 11 (9.84 $\pm$ 1.25) S cm^{-1} which is the highest among doped films in this work (**Figure 3d**). PClBD with 75 mol% doping with N-DMBI has the highest σ of 6.8 S cm$^{-1,}$ which is higher than for TP-DMBI-doped PClBD. The broader range of trap structures and energies for PDTz discussed in the electrochemistry section might have increased the relative σ enhancement from TP-DMBI on PDTz compared to PClBD. However, the larger Seebeck coefficient of TP-DMBI doped PClBD (560 vs 400 μV K^{-1}) at a comparable conductivity (1 S/cm) contributes to a higher *PF* of 32 μW m^{-1} K^{-2}; only a few n-type polymers show *PF* of over 1 μW m^{-1} K^{-2},[32] so the performance of TP-DMBI doped films is outstanding. PClBD doped by 30, 50, 75 and 100 mol% TP-DMBI have Seebeck coefficients of -560, -220, -170 and -410 μV m^{-1} K^{-1}, respectively; The corresponding *S* of PClBD doped by N-DMBI at the same doping levels are -410, -150, -21 and 23 μV m^{-1} K^{-1} (**Figure 3**). TP-DMBI- doped PDTz also exhibited slightly larger *S* than when doped with N-DMBI, though the σ accompanying those values of *S* are several times higher than with N-DMBI doping. Benefitting from the higher *S*, TP-DMBI-doped PDTz exhibits the highest *PF* of 15 μW m^{-1} K^{-2} which is much larger than the highest *PF* (2.5 μW m^{-1} K^{-2}) of N-DMBI-doped PDTz. The 1:1 mixture of PClBD and PDTz doped by N-DMBI and TP-DMBI all show relatively lower σ of 2.6 and 2.7 S cm^{-1}, respectively; this may be caused by phase separation between polymers in the presence of dopants. A high *PF* of 20 μW m^{-1} K^{-2} is achieved by the TP-DMBI doped mixture of PClBD and PDTz and was again the result of several times higher *S* at comparable conductivity (Figure S11).

We further compared the *S* of N-DMBI and TP-DMBI doped films at similar σ levels (**Figure 4a and b**). Both of PClBD and PDTz doped by TP-DMBI show larger *S* than

when doped by N-DMBI. It was suggested that larger *S* could be associated with higher polymer host-dopant distance.[10a] Moreover, the better miscibility between polymers and TP-DMBI that has been confirmed by atomic force microscopy (AFM) images (**Figure 6**) and X-ray diffraction (XRD) measurements (Figure S8) could also contribute to the higher Seebeck coefficient.[33] The time-dependent thermoelectric voltage response under different temperature gradients ΔT further illustrates that TP-DMBI doped polymer films have larger output thermoelectric voltages at unit temperature gradient bias than those of N-DMBI doped polymers (Figure S7), and suggests the thermoelectric voltages only derive from an electronic contribution, not from ionic contributions.[19]

Temperature-dependent electrical conductivity measurements were used to reveal the relationship between σ and temperature. As shown in **Figure 4**, 50 mol% doped polymer films exhibit increasing σ with rising temperatures from about 25 ℃ to 120 ℃. The Arrhenius plots of PClBD and PDTz doped by N-DMBI (**Figure 4c and d**) are not very linear at high temperature, perhaps because those doped films are not stable at considerably elevated temperature. The TP-DMBI-doped films show much more linear reciprocal temperature dependence of σ. According to the Arrhenius equation, the apparent activation energies (E_a) of carrier hopping for PClBD, PDTz doped by N-DMBI are 340 and 480 meV, respectively; and PClBD, PDTz doped by TP-DMBI are 300 and 320 meV (**Figure 4f and g**), respectively. The lower E_a of TP-DMBI doped polymer films could be because of the better miscibility between polymers and TP-DMBI, and lower disorder of TP-DMBI compared to N-DMBI as discussed below. The values of the activation energy divided by the average temperature of the measurements are 1040, 1450, 900 and 970 μV K^{-1}. The E_a for the N-DMBI and TP-DMBI doped mixtures of PClBD and PDTz are 310 and 370 meV; the corresponding values of the

activation energy divided by the average temperature are 940 and 1110 μV K^{-1}. These are somewhat higher than the measured Seebeck coefficients, indicating a barrier to site-to-site hopping, but are of the same order of magnitude as *S*.

In the formulation $\sigma = ne\mu$, where n is carrier density, e is electron charge and μ is the corresponding carrier mobility, σ is positively related to μ and n of polymer films.[34] To reveal the electron mobilities of pristine and doped polymer films, organic field effect transistors with top-gate/bottom-contact (TGBC) configuration were prepared. The electron mobilities were calculated according to the transfer curves and summarized in Table S3. Pristine PClBD and PDTz show electron mobilities (μ_e) of 0.14±0.01 and 0.20±0.03 cm^2 V^{-1} s^{-1} (**Figure 5** and Table S3), with the lower LUMO energy levels likely contributing to the higher μ_e of PDTz. The I_{on}/I_{off} of PDTz (**Figure 5e**) is 5000-10000 which is much higher than the 200 of PClBD (**Figure 5a**). The μ_e for N-DMBI doped PClBD and PDTz are 0.16±0.01 and 0.26±0.01 cm^2 V^{-1} s^{-1}. The corresponding μ_e of TP-DMBI doped PClBD and PDTz are 0.51±0.02 and 0.44±0.04 cm^2 V^{-1} s^{-1}. The higher mobility, if maintained at higher doping levels, should be associated with higher power factors because it allows increased charge transport for a given difference between Fermi and transport energies. The mixed films of PClBD and PDTz doped by N-DMBI and TP-DMBI have μ_e of 0.36±0.04 and 0.43±0.09 cm^2 V^{-1} s^{-1}, respectively.

The surface morphology of polymer films was investigated by AFM (**Figure 6**). TP-DMBI doped PClBD, PDTz and mixture of PClBD and PDTz present more dense bundles of entangled fine fibrils with smaller sizes than films doped by N-DMBI, especially for TP-DMBI doped PDTz and the mixture films. Furthermore, the RMS roughnesses for TP-DMBI doped PClBD, PDTz and mixture films are 2.56, 1.29 and

1.70 nm, respectively, which are smaller than those doped by N-DMBI, TP-DMBI doped polymer films showed smaller sized fiber-like aggregations, indicating better miscibility of TP-DMBI with polymers.

The larger mobilities of TP-DMBI and mixed films compared to single PClBD or PDTz films alone or with N-DMBI may be because of better surface morphology and smaller root mean square (RMS) roughness, as was shown in **Figure 6**, a sign of good miscibility. Smooth surface morphology and ordered arrangement of polymer molecules are critical for electron transport.[35]

Grazing incidence X-ray scattering (GIXRS) was performed to examine the microstructures of polymer films which were prepared in a similar manner to the doped devices. The strong (100), (200) and weak (300) diffraction peaks in the out-of-plane directions were observed, and there were no (010) diffraction peaks associated with π-π stacking observed for both of PClBD and PDTz (Figure S8), indicating the conjugated backbones of polymers tend to assume edge-on orientation packing.[35] The corresponding lamellar *d*-spacing distances are 2.96 and 3.13 nm; the results are in agreement with the values of other BDOPV-based polymers measured by 2D grazing incidence wide-angle x-ray scattering (GIWAXS).[11c] N-DMBI doped PClBD shows a (010) diffraction peak at 25.74° with π-π stacking distance of 3.46 Å, indicating face-on packing for some polymer molecules formed; the corresponding lamellar *d*-spacing distance extends to 3.69 nm because N-DMBI disorders the molecular packing. The lamellar *d*-spacing of TP-DMBI doped PClBD slightly increases to 3.13 nm. For N-DMBI doped PDTz, when the dopant mole ratio increased from 0 to 100 mol%, the (300) diffraction peak nearly disappeared; For TP-DMBI doped PDTz, when the dopant mole ratio increased from 0 to 100 mol%, especially from 30 mol% to 100 mol%, the

(300) diffraction peak is still observed (Figure S8). The results suggest that N-DMBI disrupts the polymer molecular packing much more than does TP-DMBI, further confirming that TP-DMBI shows better miscibility with polymers than N-DMBI.[36]

3. Summary and Conclusion

In conclusion, the matching of polymer structures and dopant sidechains can enhance the performance of n-type organic thermoelectrics. TP-DMBI doped thin films lead to much higher electron mobilities than N-DMBI doping, with the highest electron mobility of 0.53 $cm^2 V^{-1} s^{-1}$. All of the doped films present reasonably high electrical conductivity, suggesting A-A type polymers are suitable for organic thermoelectrics. The highest electrical conductivity from this study of 11 S cm^{-1} is obtained from 75 mol% TP-DMBI doped PDTz. The highest electrical conductivity value of doped PDTz is larger than the value for doped PClBD, indicating that polymers with lower ratios of single bonds in their backbones can have enhanced electrical conductivity. More importantly, TP-DMBI doped polymer films show much higher Seebeck coefficient at the same doping levels or similar conductivity levels than those that are N-DMBI doped, contributing to high power factors of 32, 15 and 20 μW $m^{-1} K^{-2}$ for doped PClBD, PDTz and mixtures of PClBD and PDTz. The results show that 3,4,5-trimethoxy DMBI can effectively enhance the Seebeck coefficient and power factor of n-type organic thermoelectrics, and open the opportunity for polyalkoxy derivatives of N-DMBI to be explored in the future.

Acknowledgements

This work was primarily supported by the National Science Foundation, Division of Chemistry, grant numbers 1708245 and 2107360. We thank Nicholas Adams and

Tushita Mukhopadhyaya for their help with CV measurement and Baixiang Li for his help with GPC measurements. We acknowledge Lisa Pogue and Tyrel McQueen for assistance and training on the X-ray diffractometer.

Keywords: n-type organic thermoelectric • electrical conductivity and Seebeck coefficient • n-type dopant • conjugated polymer • electron mobility

[1] a) A. R. Murphy, J. M. J. Fréchet, *Chem. Rev.* **2007**, *107*, 1066; b) J. Li, K. Pu, *Chem. Soc. Rev.* **2019**, *48*, 38; c) T. K. Das, S. Prusty, *PPTEn* **2012**, *51*, 1487.
[2] B. Lüssem, C.-M. Keum, D. Kasemann, B. Naab, Z. Bao, K. Leo, *Chem. Rev.* **2016**, *116*, 13714.
[3] B. Russ, A. Glaudell, J. J. Urban, M. L. Chabinyc, R. A. Segalman, *Nat. Rev. Mater.* **2016**, *1*, 16050.
[4] H. Li, J. Song, J. Xiao, L. Wu, H. E. Katz, L. Chen, *Adv. Funct. Mater.* **2020**, *30*, 2004378.
[5] H. Li, M. E. DeCoster, R. M. Ireland, J. Song, P. E. Hopkins, H. E. Katz, *J. Am. Chem. Soc.* **2017**, *139*, 11149.
[6] Y. Lu, Z.-D. Yu, H.-I. Un, Z.-F. Yao, H.-Y. You, W. Jin, L. Li, Z.-Y. Wang, B.-W. Dong, S. Barlow, E. Longhi, C.-a. Di, D. Zhu, J.-Y. Wang, C. Silva, S. R. Marder, J. Pei, *Adv. Mater.* **2021**, *33*, 2005946.
[7] H. Li, M. E. DeCoster, C. Ming, M. Wang, Y. Chen, P. E. Hopkins, L. Chen, H. E. Katz, *Macromolecules* **2019**, *52*, 9804.
[8] J. Ding, Z. Liu, W. Zhao, W. Jin, L. Xiang, Z. Wang, Y. Zeng, Y. Zou, F. Zhang, Y. Yi, Y. Diao, C. R. McNeill, C.-a. Di, D. Zhang, D. Zhu, *Angew. Chem. Int. Ed.* **2019**, *58*, 18994.
[9] T. Park, C. Park, B. Kim, H. Shin, E. Kim, *Energy Environ. Sci.* **2013**, *6*, 788.
[10] a) J. Liu, G. Ye, B. v. d. Zee, J. Dong, X. Qiu, Y. Liu, G. Portale, R. C. Chiechi, L. J. A. Koster, *Adv. Mater.* **2018**, *30*, 1804290; b) J. Liu, Y. Shi, J. Dong, M. I. Nugraha, X. Qiu, M. Su, R. C. Chiechi, D. Baran, G. Portale, X. Guo, L. J. A. Koster, *ACS Energy Lett.* **2019**, *4*, 1556; c) C.-Y. Yang, M.-A. Stoeckel, T.-P. Ruoko, H.-Y. Wu, X. Liu, N. B. Kolhe, Z. Wu, Y. Puttisong, C. Musumeci, M. Massetti, H. Sun, K. Xu, D. Tu, W. M. Chen, H. Y. Woo, M. Fahlman, S. A. Jenekhe, M. Berggren, S. Fabiano, *Nat. Commun.* **2021**, *12*, 2354; d) C. Dong, S. Deng, B. Meng, J. Liu, L. Wang, *Angew. Chem. Int. Ed.* **2021**, *60*, 16184.
[11] a) O. Bardagot, P. Kubik, T. Marszalek, P. Veyre, A. A. Medjahed, M. Sandroni, B. Grévin, S. Pouget, T. Nunes Domschke, A. Carella, S. Gambarelli, W. Pisula, R. Demadrille, *Adv. Funct. Mater.* **2020**, *30*, 2000449; b) X. Zhao, D. Madan, Y. Cheng, J. Zhou, H. Li, S. M. Thon, A. E. Bragg, M. E. DeCoster, P. E. Hopkins, H. E. Katz, *Adv. Mater.* **2017**, *29*, 1606921; c) J. Han, C. Ganley, Q. Hu, X. Zhao, P. Clancy, T. P. Russell, H. E. Katz, *Adv. Funct. Mater.* **2021**, *31*, 2010567.
[12] K. Feng, H. Guo, J. Wang, Y. Shi, Z. Wu, M. Su, X. Zhang, J. H. Son, H. Y. Woo, X. Guo, *J. Am. Chem. Soc.* **2021**, *143*, 1539.
[13] X. Yan, M. Xiong, J. T. Li, S. Zhang, Z. Ahmad, Y. Lu, Z. Y. Wang, Z. F. Yao, J. Y. Wang, X. Gu, T. Lei, *J. Am. Chem. Soc.* **2019**, *141*, 20215.
[14] a) Y. Lu, Z. D. Yu, R. Z. Zhang, Z. F. Yao, H. Y. You, L. Jiang, H. I. Un, B. W. Dong, M. Xiong, J. Y. Wang, J. Pei, *Angew. Chem. Int. Ed.* **2019**, *58*, 11390; b) H. Chen, M. Moser, S. Wang, C. Jellett, K. Thorley, G. T. Harrison, X. Jiao, M. Xiao, B.

Purushothaman, M. Alsufyani, H. Bristow, S. De Wolf, N. Gasparini, A. Wadsworth, C. R. McNeill, H. Sirringhaus, S. Fabiano, I. McCulloch, *J. Am. Chem. Soc.* **2021**, *143*, 260.
[15] Y. Wang, M. Nakano, T. Michinobu, Y. Kiyota, T. Mori, K. Takimiya, *Macromolecules* **2017**, *50*, 857.
[16] a) J. Han, H. Fan, Q. Zhang, Q. Hu, T. P. Russell, H. E. Katz, *Adv. Funct. Mater.* **2021**, *31*, 2005901; b) C.-Y. Yang, W.-L. Jin, J. Wang, Y.-F. Ding, S. Nong, K. Shi, Y. Lu, Y.-Z. Dai, F.-D. Zhuang, T. Lei, C.-A. Di, D. Zhu, J.-Y. Wang, J. Pei, *Adv. Mater.* **2018**, *30*, 1802850.
[17] Y. Wang, K. Takimiya, *Adv. Mater.* **2020**, *32*, 2002060.
[18] a) H.-I. Un, S. A. Gregory, S. K. Mohapatra, M. Xiong, E. Longhi, Y. Lu, S. Rigin, S. Jhulki, C.-Y. Yang, T. V. Timofeeva, J.-Y. Wang, S. K. Yee, S. Barlow, S. R. Marder, J. Pei, *Adv. Energy Mater.* **2019**, *9*, 1900817; b) D. Yuan, D. Huang, C. Zhang, Y. Zou, C.-a. Di, X. Zhu, D. Zhu, *ACS Appl. Mater. Inter.* **2017**, *9*, 28795.
[19] Y. Lu, Z.-D. Yu, Y. Liu, Y.-F. Ding, C.-Y. Yang, Z.-F. Yao, Z.-Y. Wang, H.-Y. You, X.-F. Cheng, B. Tang, J.-Y. Wang, J. Pei, *J. Am. Chem. Soc.* **2020**, *142*, 15340.
[20] X. Yin, F. Zhong, Z. Chen, C. Gao, G. Xie, L. Wang, C. Yang, *Chem. Eng. J.* **2020**, *382*, 122817.
[21] B. D. Naab, S. Guo, S. Olthof, E. G. B. Evans, P. Wei, G. L. Millhauser, A. Kahn, S. Barlow, S. R. Marder, Z. Bao, *J. Am. Chem. Soc.* **2013**, *135*, 15018.
[22] X.-Q. Zhu, M.-T. Zhang, A. Yu, C.-H. Wang, J.-P. Cheng, *J. Am. Chem. Soc.* **2008**, *130*, 2501.
[23] J. Han, D. Yang, Y. Wang, D. Ma, W. Qiao, Z. Y. Wang, *J. Mater. Chem. C* **2018**, *6*, 10838.
[24] B. M. Reinhard, G. Niedner-Schatteburg, *J. Chem. Phys.* **2003**, *118*, 3571.
[25] a) Y. Zeng, W. Zheng, Y. Guo, G. Han, Y. Yi, *J. Mater. Chem. A* **2020**, *8*, 8323; b) L. Qiu, J. Liu, R. Alessandri, X. Qiu, M. Koopmans, Remco W. A. Havenith, S. J. Marrink, R. C. Chiechi, L. J. Anton Koster, J. C. Hummelen, *J. Mater. Chem. A* **2017**, *5*, 21234.
[26] P. Wei, J. H. Oh, G. Dong, Z. Bao, *J. Am. Chem. Soc.* **2010**, *132*, 8852.
[27] B. D. Naab, X. Gu, T. Kurosawa, J. W. F. To, A. Salleo, Z. Bao, *Adv. Electron. Mater.* **2016**, *2*, 1600004.
[28] J. L. Bredas, G. B. Street, *Acc. Chem. Res.* **1985**, *18*, 309.
[29] C. Deibel, T. Strobel, V. Dyakonov, *Adv. Mater.* **2010**, *22*, 4097.
[30] K. Shi, F. Zhang, C. A. Di, T. W. Yan, Y. Zou, X. Zhou, D. Zhu, J. Y. Wang, J. Pei, *J. Am. Chem. Soc.* **2015**, *137*, 6979.
[31] S.-G. Chen, H. M. Branz, S. S. Eaton, P. C. Taylor, R. A. Cormier, B. A. Gregg, *J. Phys. Chem. B* **2004**, *108*, 17329.
[32] Y. Lu, J.-Y. Wang, J. Pei, *Chem. Mater.* **2019**, *31*, 6412.
[33] C. J. Boyle, M. Upadhyaya, P. Wang, L. A. Renna, M. Lu-Díaz, S. Pyo Jeong, N. Hight-Huf, L. Korugic-Karasz, M. D. Barnes, Z. Aksamija, D. Venkataraman, *Nat. Commun.* **2019**, *10*, 2827.
[34] K. S. Novoselov, A. K. Geim, S. V. Morozov, D. Jiang, Y. Zhang, S. V. Dubonos, I. V. Grigorieva, A. A. Firsov, *Science* **2004**, *306*, 666.
[35] K. Guo, J. Bai, Y. Jiang, Z. Wang, Y. Sui, Y. Deng, Y. Han, H. Tian, Y. Geng, *Adv. Funct. Mater.* **2018**, *28*, 1801097.
[36] C.-Y. Yang, Y.-F. Ding, D. Huang, J. Wang, Z.-F. Yao, C.-X. Huang, Y. Lu, H.-I. Un, F.-D. Zhuang, J.-H. Dou, C.-a. Di, D. Zhu, J.-Y. Wang, T. Lei, J. Pei, *Nat. Commun.* **2020**, *11*, 3292.

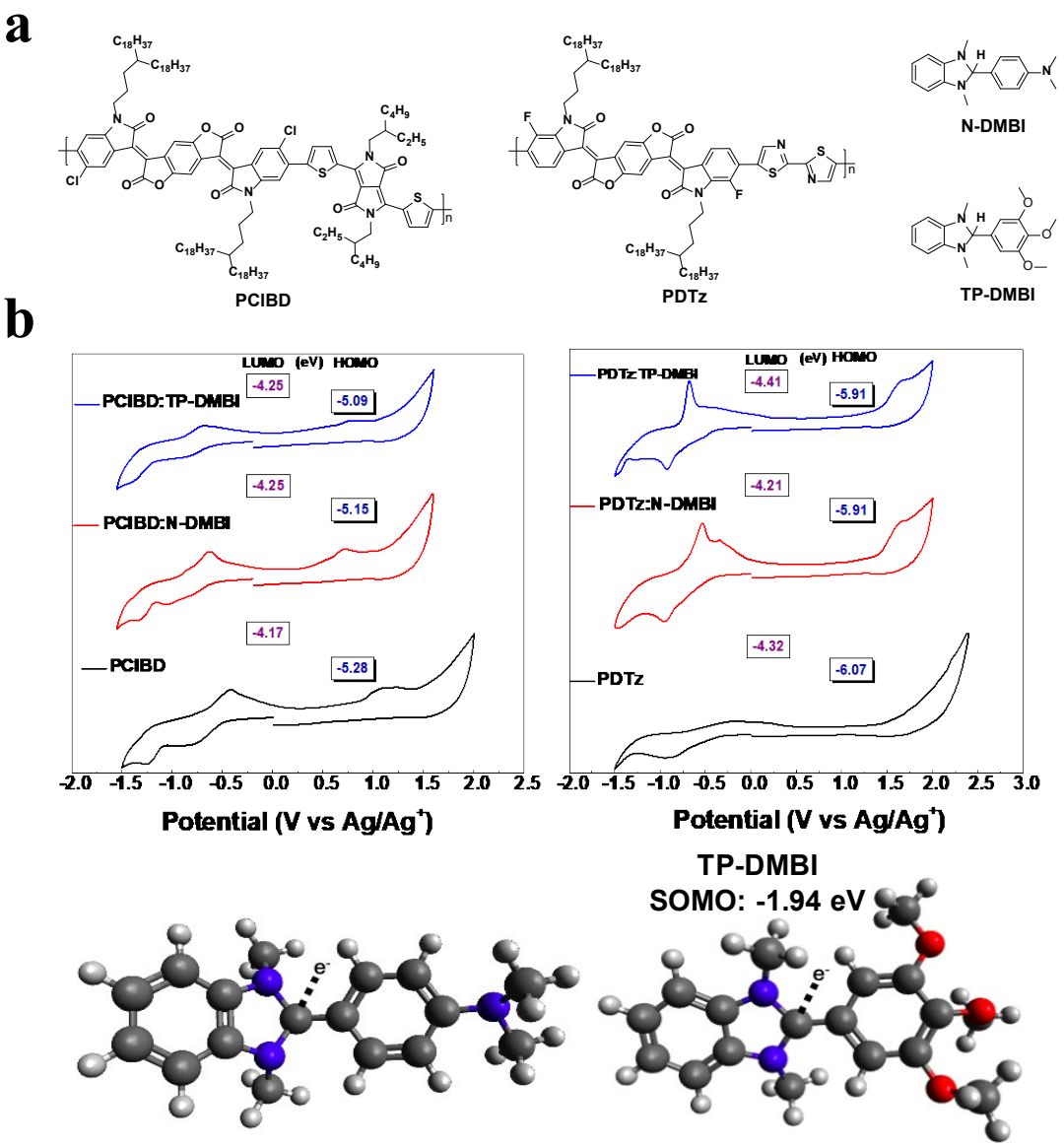

Figure 1. (a) Chemical structures of polymers and dopants used in this work. (b) Cyclic voltammograms and energy levels of PClBD and PDTz doped with 50 mol% N-DMBI and 50 mol% TP-DMBI, respectively. (c) Atomic-scale representation and the SOMO energy levels of radical N-DMBI˙ and TP-DMBI˙.

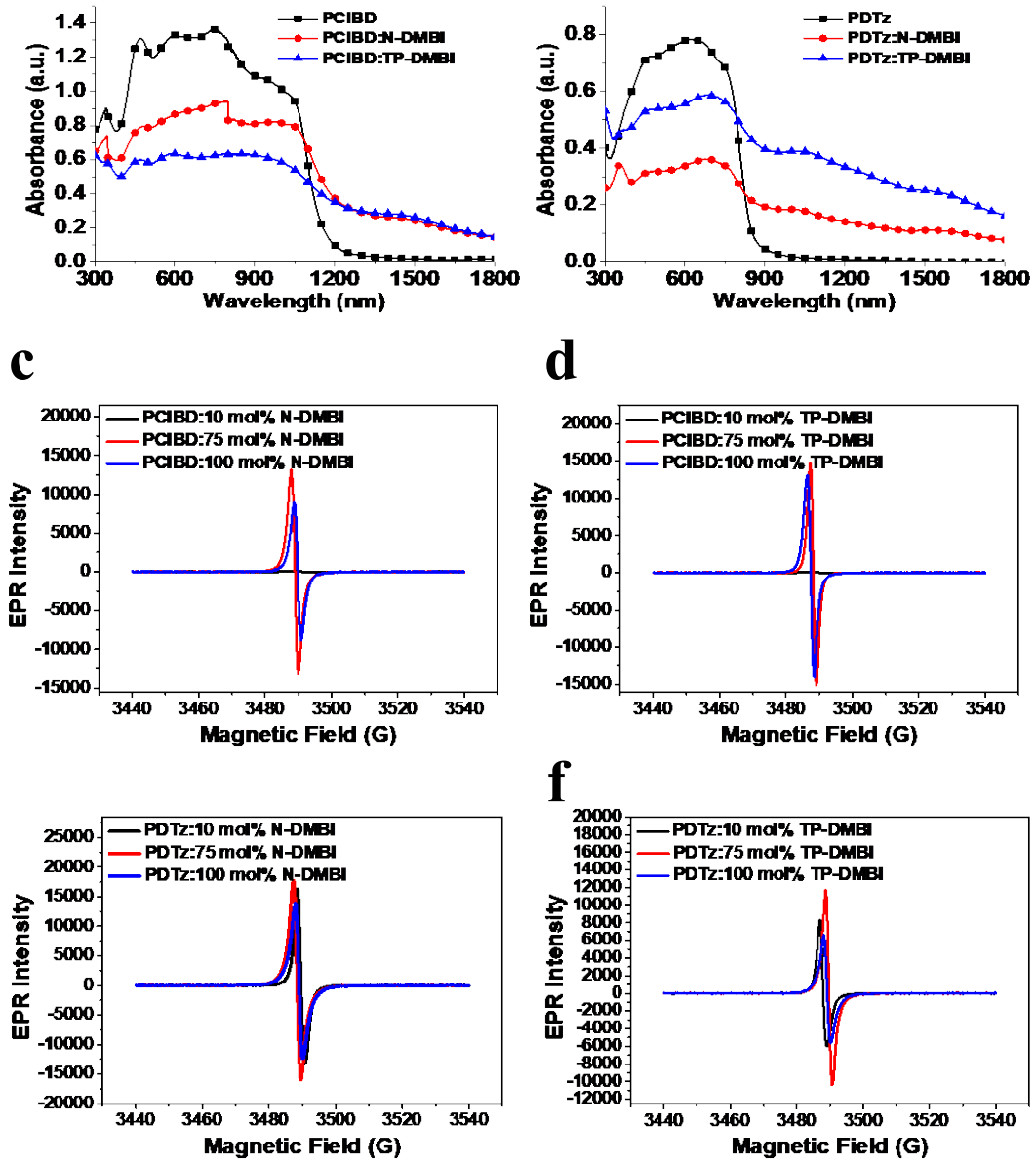

Figure 2. Absorption spectra of pristine (a) PClBD, (b) PDTz doped by 50 mol% N-DMBI and 50 mol% TP-DMBI films. EPR spectra of PClBD doped by various concentrations of (c) N-DMBI and (d) TP-DMBI. EPR spectra of PDTz doped by various concentrations of (e) N-DMBI and (f) TP-DMBI solution.

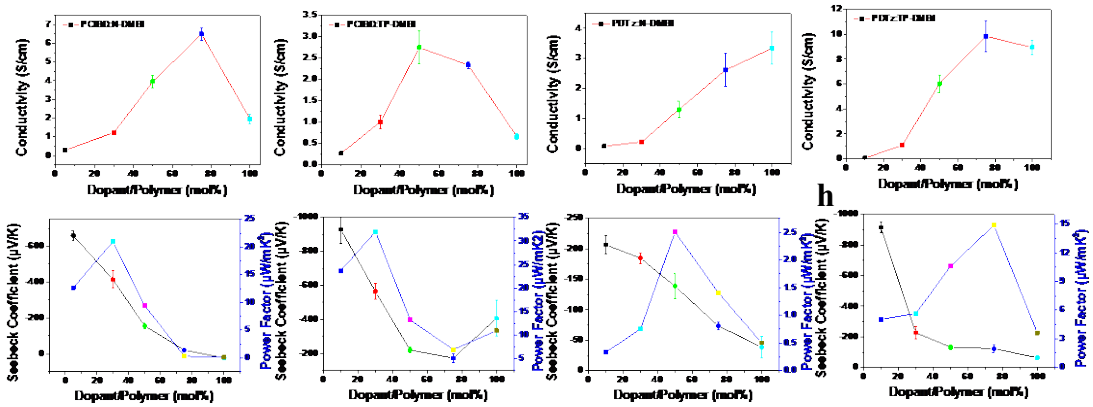

Figure 3. Electrical conductivity of PClBD (PDTz) doped by (a) (c) N-DMBI, (b) (d) TP-DMBI. Seebeck coefficient and power factors of PClBD (PDTz) doped by (e) (g) N-DMBI, (f) (h)TP-DMBI.

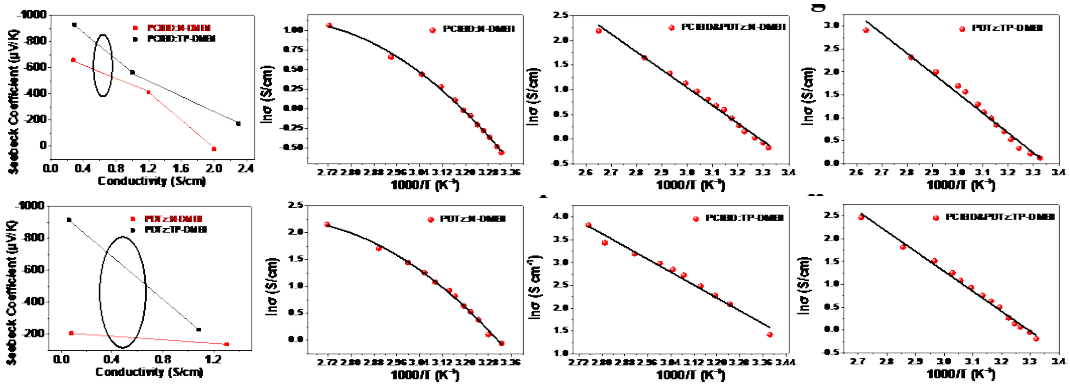

Figure 4. Experimental *S*-σ plots of N-DMBI and TP-DMBI doped (a) PClBD and (b) PDTz. Temperature-dependent electrical conductivity values of N-DMBI (TP-DMBI) doped (c) (f) PClBD, (d) (g) PDTz and (e) (h) 1:1 mixture of PClBD and PDTz.

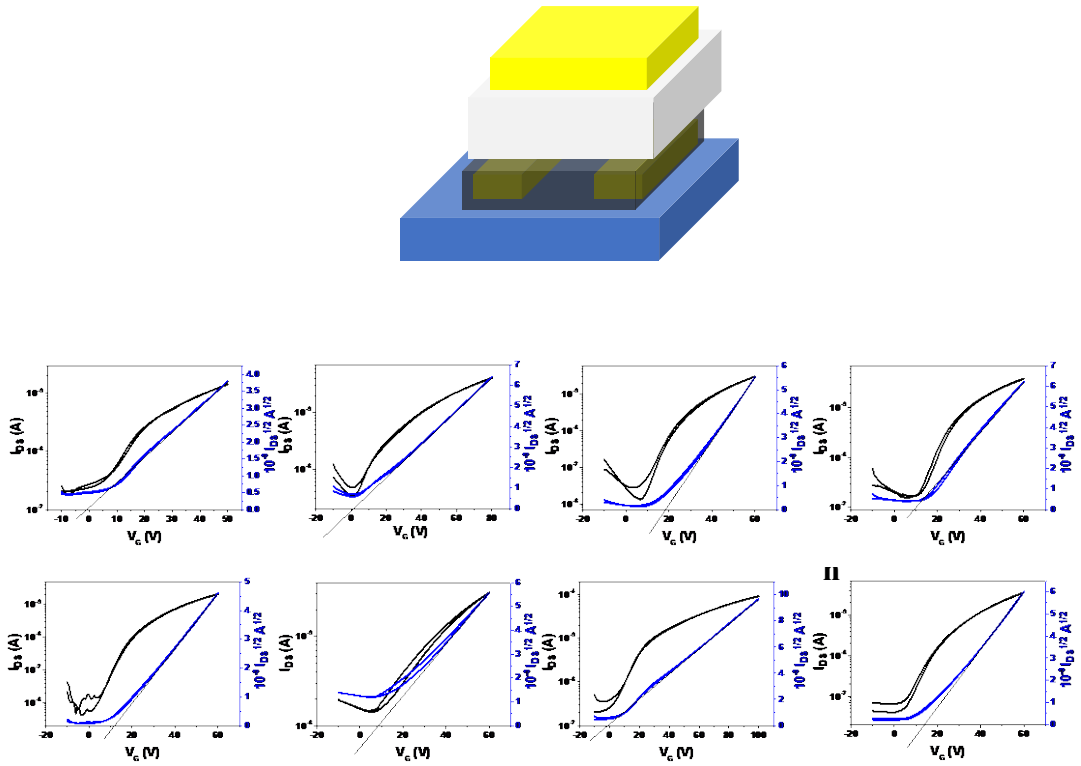

Figure 5. The device diagram of TGBC devices and OFET transfer curves of (a) PClBD, PClBD doped by (b) N-DMBI, (c) TP-DMBI, (d) mixture of PClBD and PDTz doped by N-DMBI, (e) PDTz, PDTz doped by (f) N-DMBI, (g) TP-DMBI and (h) mixture of PClBD and PDTz doped by TP-DMBI. The slopes of the straight lines shown were set equal to sqrt $(W/2L)\mu C_i$ for mobility calculation. Minor nonlinearities, possibly indicating μ dependent on V_G, are observed near the x-intercepts (V_T). Mobility would decrease (only near V_T) to about 2/3 of the values listed in the text for plots 5c, 5f, and 5h, and would have smaller local variations near V_T in plots 5a, 5b, and 5g.

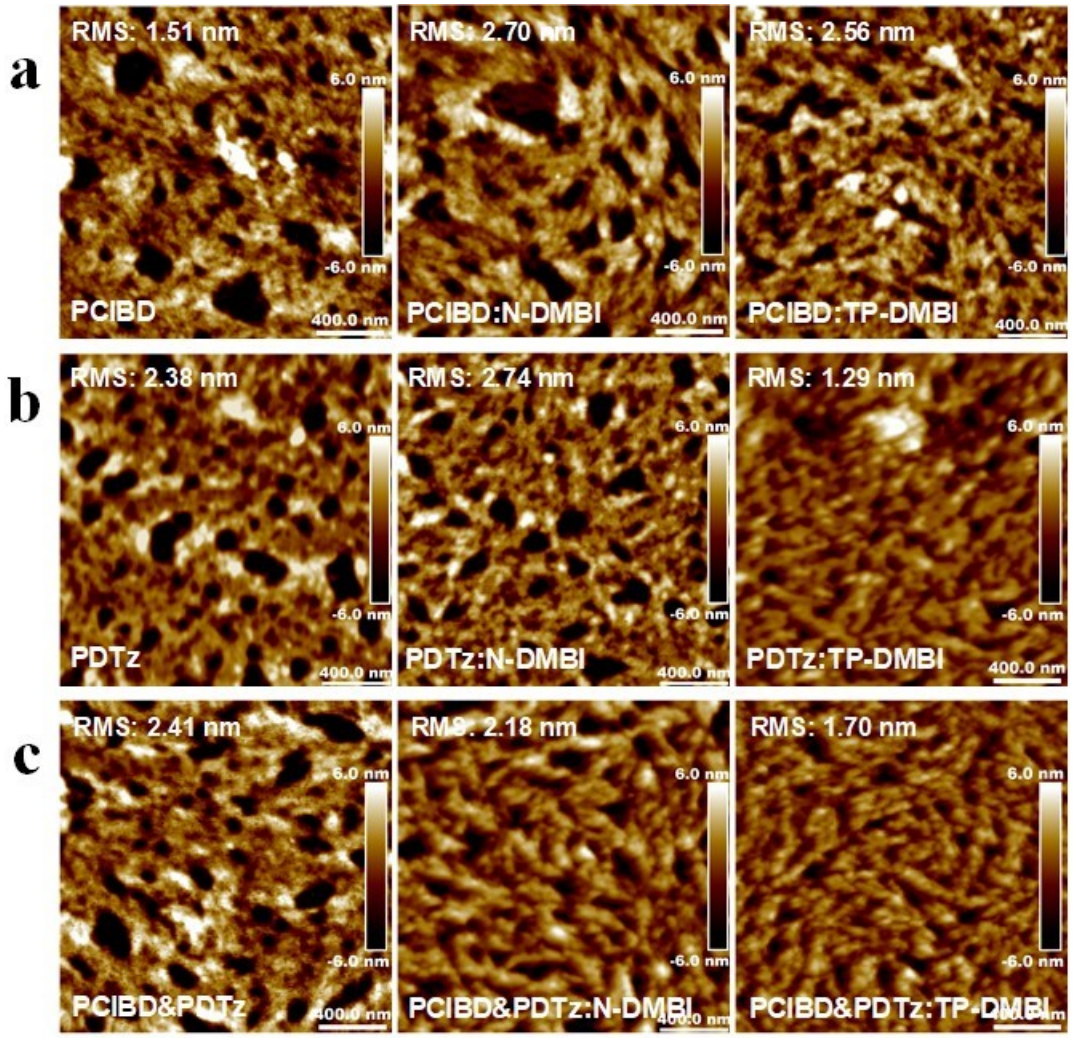

Figure 6. (a) (b) (c) AFM height images of polymer PClBD (PDTz) (mixture of PClBD and PDTz), PClBD (PDTz) (mixture of PClBD and PDTz), doped with 50 mol% N-DMBI and 50 mol% TP-DMBI (2 μm x 2 μm).

Entry for the Table of Contents

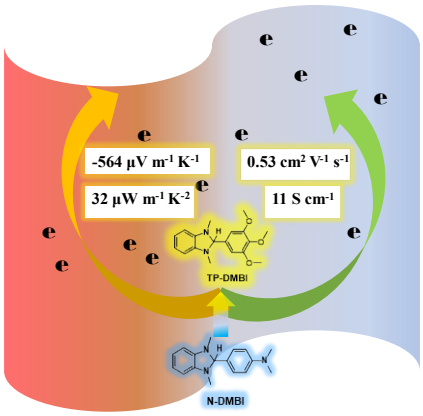

Two n-type conjugated polymers with different backbones and a n-type dopant 1,3-dimethyl-2-(3,4,5-trimethoxyphenyl)-2,3-dihydro-1H-benzo[d]imidazole (TP-DMBI) are synthesized, and electron mobility of 0.53 cm^2 V^{-1} S^{-1}, electrical conductivity of 11 S cm^{-1} and power factor 32 μW m^{-1} K^{-2} for n-type organic thermoelectrics are achieved by TP-DMBI doped films, which out-perform N-DMBI doped films.